High-pressure and high-temperature x-ray absorption study of liquid and solid gallium

Lucia Comez and Andrea Di Cicco
INFM, Dipartimento di Matematica e Fisica, Università degli Studi di Camerino, Via Madonna delle Carceri, 62032 Camerino (MC), Italy

Jean Paul Itié and Alain Polian
LURE and Laboratoire de Physique des Milieux Condensés, Université Pierre et Marie Curie, T13 E4, 4 place Jussieu, F-75252 Paris CEDEX 05, France

(Received 21 July 2000; revised manuscript received 2 July 2001; published 13 December 2001)

Good quality extended x-ray absorption fine structure (EXAFS) spectra near the Ga *K* edge have been collected in wide pressure and temperature ranges (namely 0–16 GPa, 298–498 K) using the dispersive setup installed at the LURE synchrotron radiation facility and diamond anvil cell as pressure device. Energy dispersive x-ray diffraction data have been also measured in similar thermodynamical conditions. EXAFS spectra are shown to be sensitive to phase transitions occurring at high pressures and temperatures. Occurrence of stable and metastable phases and location of the coexistence lines are discussed in light of the results obtained using both experimental techniques. The phase diagram of pure gallium has been extended considering present experimental results. EXAFS data-analysis is performed using advanced *ab initio* methods (GNXAS). Accurate information about local structure in solid and liquid gallium at extreme conditions is obtained. The short-range two-body distribution functions are reconstructed by EXAFS for liquid and solid gallium as a function of pressure and temperature.

DOI: 10.1103/PhysRevB.65.014114 PACS number(s): 61.10.Ht, 61.25.Mv, 62.50.+p

I. INTRODUCTION

Gallium is a metal which is known to be polymorphic showing several phase transitions and metastable modifications as a function of pressure and temperature.[1–8] The melting temperature at ambient pressure of the stable phase Ga(I) (or α-Ga) is particularly low ($T_m = 302.9$ K) and extreme undercooling of the liquid can be easily obtained.[2,3] Moreover, gallium is an ice-type element where the density of the liquid phase at ambient pressure exceeds of about 3% that of the stable Ga(I) phase. Therefore, gallium melts upon application of pressure at room temperature (slope of the coexistence line I liquid $\delta T/\delta P \sim -23$ K/GPa). It is then possible to investigate liquid gallium in a broad range of temperatures and pressures without too complicated high-temperature–high-pressure experimental equipments.

In the past, the part of the Ga phase diagram including the 233–423 K temperature and 0–7.5 GPa pressure ranges has been explored by differential thermal analysis and x-ray diffraction measurements.[1,4] The liquid-solid Ga(II) transition is located at about 2.0 GPa at room temperature. The average structure of liquid gallium (l-Ga) has been studied at ambient pressure using neutron and x-ray diffraction as reported in several previous publications (see, for example, Refs. 9,10). It was found that the principal peak of the structure factor $S(q)$ is asymmetric and has a shoulder on the high-q side just above the melting temperature. This anomalous feature merges into the principal peak increasing its asymmetry at very high temperature while develops into a well-defined peak in the supercooled liquid.[11,12] Several computer simulations have been performed in a wide range of temperature at ordinary pressure in order to clarify the origin of the anomalies in the observed structure factors and improve the knowledge of the electronic properties of liquid gallium (see, for example, Refs. 13,14). The average structure of l-Ga has been simulated by using realistic interatomic pair pseudopotentials which can explain the asymmetry of the $S(q)$.[15–17] Hafner *et al.*[17] attributed the $S(q)$ anomalous shape of liquid Ga to a change of the curvature of the pair potential corresponding to the nearest-neighbor distance. Tsay and coworkers[18–20] gave a structural interpretation ascribing the $S(q)$ anomalies to the simultaneous presence of clusters of atoms of different size and geometry.

The only experimental investigations of liquid gallium at high temperatures and pressures have been performed using x-ray diffraction[21,22] up to 1570 K, 0.07 GPa (Ref. 21) and up to 393 K, 6.1 GPa on the high-pressure side.[22] The nearest neighbor distance turned to be almost constant, whereas the coordination number decreases as a function of temperature[21] and increases as a function of pressure.[22]

For what concerns solid Ga at high pressure, Schulte and Holzapfel[7] have interpreted their energy-dispersive x-ray diffraction (EDXD) measurements as due to the existence of various competing phases up to around 15 GPa (at room temperature) when Ga finally transforms to Ga(III) phase. However, the problem of an unambiguous determination of the intermediate pressure regime in Ga is still open as also indicated by the authors themselves. The Ga(III) phase is the stable phase at room temperature from 15 GPa up to about 75 GPa. At very high-pressure, different assignments of the Ga(III)-Ga(IV) (fcc) transition ranging from the extrapolation reported in Ref. 7 (75 GPa) and recent EDXD measurements showing a ''continuous'' transition above 120 GPa (Ref. 8) have been suggested.

So far, no x-ray absorption spectroscopy (XAS) measurements have been performed as a function of pressure and temperature on pure gallium. In recent times, it has been shown that reliable structural information can be obtained by

XAS data collected using the energy-dispersive setup and diamond anvil cells (DAC's) as pressure devices.[23,24] Large-volume cells have been also used in the 0–7 GPa and 300–1200 K pressure and temperature ranges on standard XAS beamlines providing very good quality spectra in extreme conditions.[25] The unique short-range sensitivity of the XAS technique has been exploited providing unambiguous results about the local structure, complementing those obtained using diffraction techniques.[23–25]

The capability of the XAS to give quantitative information on the radial distribution function is considerably improved due to the advances in the data interpretation.[26] The *ab initio* multiple-scattering approach for data analysis contained in the GNXAS method can be successfully used to determine the local two-body and even three-body distribution functions both in liquid and solid phases (see, for example, Refs. 23,26–29).

In this work, we present energy dispersive XAS and energy dispersive x-ray diffraction measurements on solid and liquid gallium in a wide pressure and temperature domain (0–16 GPa and 298–498 K). The main purpose of this paper is to contribute to clarify the complex scenario of phase transitions of this polymorphic metal and determine the short-range local structure as a function of pressure and temperature both for solid and liquid Ga in extreme conditions. In particular, the XAS determination of the pair distribution function of liquid gallium under extreme conditions by using the long-range constraints of complementary techniques (such as neutron or x-ray diffraction) is aimed to stimulate new theoretical and computational study of short-range potentials and electronic properties for polymorphic metals.

II. EXPERIMENTAL DETAILS

Ga *K*-edge XAS measurements and EDXD patterns as a function of pressure at room and high temperature were collected in two separate experiments using the dispersive setup available at LURE (D11 and DW11A beamlines)[30,31] and synchrotron radiation emitted by the DCI storage ring operating at 1.85 GeV with typical currents of 300 mA.

XAS spectra covered the 0–8.2 GPa, the 0–11.8 GPa, and 0–16 GPa pressure ranges at room temperature $T=378$ K and $T=498$ K, respectively. A standard diamond anvil cell (DAC) was used as pressure device. The cell was equipped with an external heater for the high-temperature measurements. Pure gallium was loaded into the cell equipped with stainless steel gaskets without pressure-transmitting medium. The size of the sample (hole of the gasket) was about 150 μm. Particular care was taken to improve the quality of the spectra minimizing the appearance of strong Bragg peaks from the diamonds by optimizing the position of the cell and of the two diamonds. Pressure was measured before and after each XAS scan by using the standard ruby fluorescence technique with a typical 0.1 GPa error bar for the room temperature measurements. Because of the large broadening of the ruby fluorescence peak at high temperature we also used as a pressure calibrant the fluorescence of the Sm^{2+}- doped SrB_4O_7 which is nearly independent of the temperature. Temperature was monitored by a thermocouple placed on the rear of the cell with an estimated uncertainty of 5 K. The stability of the temperature during the measurements was excellent due to the mass of the cell including the heater. Low noise spectra were obtained by summing five spectra (1024 pixel data), each recorded with a total integration time of about 90 s.

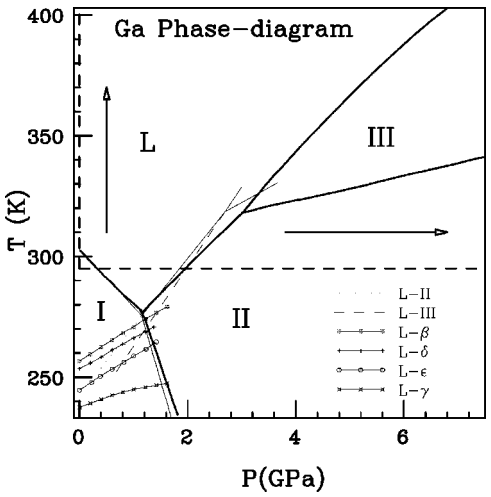

FIG. 1. Ga phase diagrams as reported in Refs. 1 (thick lines) and 4 (thin lines).

XAS experiments were performed during two separate runs and the energy scale resulted to be always a linear function of the pixel number: $E=a+bn$. The energy step b was about $b=0.853$ eV and $b=0.670$ eV while the parameter a was about $a=10203.6$ eV and $a=10289.6$ for room-temperature and high-temperature scans, respectively. The scale was obtained comparing the *K*-edge pure Ga and GaSb spectra at ambient conditions collected using the dispersive technique with analogous spectra recorded in the same conditions on a conventional spectrometer with a channel-cut (311) monochromator (beamline D42 at LURE).

EDXD patterns were recorded at a given angle using the synchrotron radiation emitted by the DCI wiggler (beamline DW11A). The angle $[\theta=5.151(1)]$ was measured using the EDXD pattern of a Cu foil at ambient conditions. Limiting pressures of the EDXD measurements were around 30, 14, and 10 GPa at 298, 378, and 498 K temperatures, respectively.

III. PHASE TRANSITIONS

In Fig. 1, we report the Ga phase diagram presented in Ref. 4 (thick lines) and the corresponding diagram reconstructed by Bosio[1] (thin lines) illustrating the previous knowledge about structural transitions of gallium under the effect of temperature and pressure. The phase diagram[4] shows the liquid-solid *l*-Ga(I), *l*-Ga(II), and *l*-Ga(III) coexistence lines and the solid-solid Ga(I)-Ga(II), Ga(II)-Ga(III) phase transitions in the 0–7.5 GPa pressure range up to 423 K. On the other hand, the phase diagram,[1] limited to a narrower region of the pressure and temperature space as compared to Ref. 4, highlights various metastable equilibrium phase boundaries (l-β, l-δ, l-ϵ, l-γ) at low temperatures

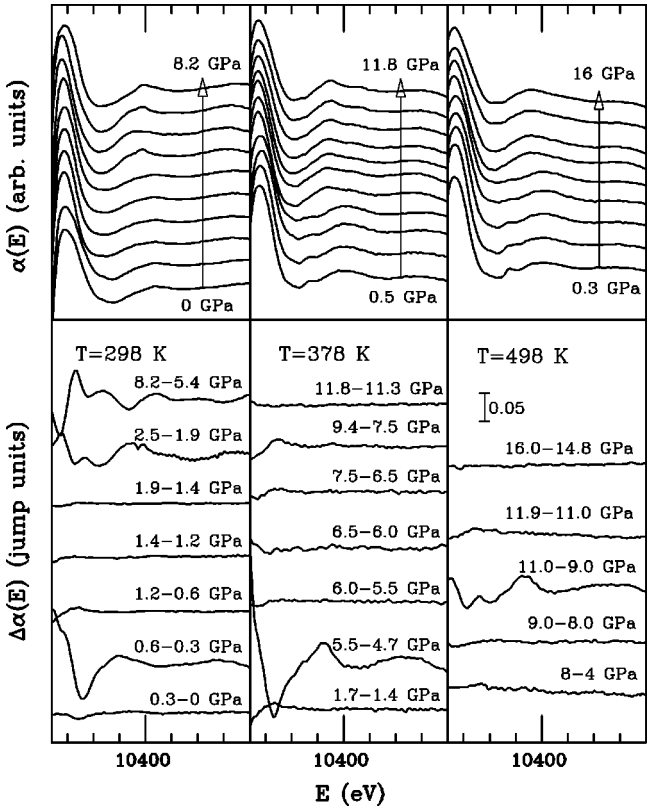

FIG. 2. Upper panels: XAS Ga *K*-edge α(E) spectra of pure gallium as a function of pressure at room temperature (ambient pressure $P=0.3$, 0.6, 1.2, 1.4, 1.9, 2.5, 3.4, 5.4, and 8.2 GPa, left panel), at $T=378$ K ($P=0.5$, 1.4, 1.7, 4.7, 5.5, 6.0, 6.5, 7.5, 9.4, 11.3, and 11.8 GPa, central panel), and $T=498$ K ($P=0.3$, 1.5, 4, 8, 9, 11, 11.9, and 14.8 GPa, right panel). Lower panels: difference signals $\Delta\alpha(E)$ of XAS spectra recorded at different pressures and temperatures.

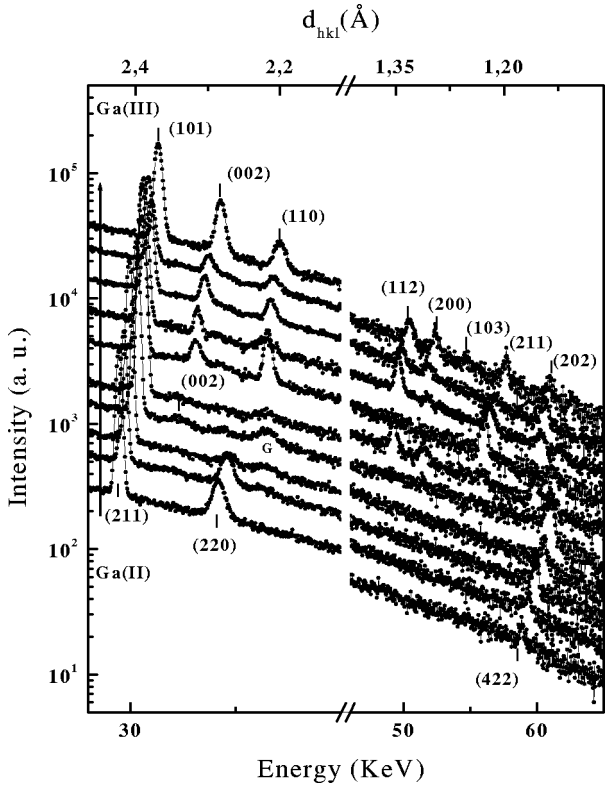

FIG. 3. Room temperature EDXD patterns of solid Ga for increasing pressure (see arrow). From the bottom to the top the EDXD patterns at 5.7, 8.6, 10.7, 14, 17, 19, 20.7, 23.3, 25.5, and 29.8 GPa are shown.

(235–265 K). A difference in the position of the triple point *L*-III-II and a slight variation in the slope of the I-II coexistence line is observed comparing the two phase diagrams. The high-pressure part of the phase diagram has been analyzed in Ref. 7.

Our Ga *K*-edge XAS spectra are presented as a function of pressure in Fig. 2 at $T=298$, 378, and 498 K. They have been found to be reproducible along the pressure upstrokes and downstrokes. The x-ray absorption coefficient $\alpha(E)$ is reported in the upper panels while differences between XAS patterns $\Delta\alpha(E)$ reflecting changes of the local structure are shown in the lower panels. Large changes in the spectra are associated with phase transitions occurring in the pressure range under investigation. At room temperature (Fig. 2, left panel) modifications are associated with the solid to liquid and liquid to solid phase transitions occurring just above 0.3 GPa (α-Ga to liquid) and 1.9 GPa (liquid to solid). Above this pressure the stable solid phase is Ga(II) but Ga(III) crystals have been observed[1] to grow in the Ga(II) stability region. The evident variation of the XAS signal at 8.2 GPa indicates that a structural modification takes place below this pressure.

For what concerns the EDXD measurements, room temperature data show the disappearance of the $S(q)$ pattern above the liquid-solid transition but no detectable Bragg peaks are observed below 5.7 GPa suggesting that a possible coexistence of different phases could take place in this pressure region. In Fig. 3 we report some of the EDXD patterns collected in the 5.7–29.8 GPa pressure range. The number of peaks detected at low pressure is insufficient to identify unambiguously the lattice structure, however, the energy positions can be compared with those predicted by using the Ga(II) and Ga(III) crystalline structures reported in the literature for these pressures. The peak assignments shown in Fig. 3 are based on this comparison. The clear structure change observed between 10.7 and 19 GPa is naturally assigned to the transformation of the Ga(II) into the Ga(III) crystalline phase in agreement with previous observations.[7] In the 5.7–10.7 pressure interval the (211), (220), and (422) interplanar distances assigned to the Ga(II) phase move progressively to higher energies as a function of pressure. Patterns in the 14–17 GPa pressure range include both Ga(II) and Ga(III) typical Bragg. New EDXD peaks, observed above 17 GPa, are assigned to the Ga(III) (101), (002),(110), (112), (200), (103), (211), and (202) interplanar distances. Lattice parameters *a* for the Ga(II) phase and *a* and *c* for the Ga(III) phase, derived from present measurements are visualized and compared with previous results[7] in Fig. 4, in the whole pressure range investigated. Lattice parameters obtained at room and higher temperatures are reported also in Table I.

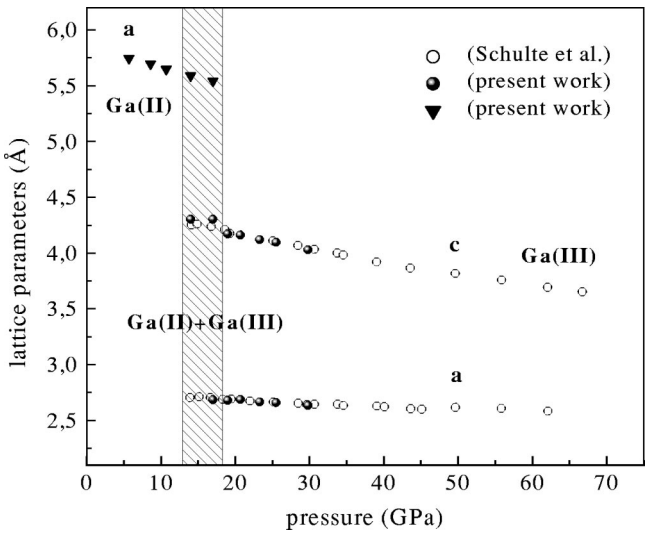

FIG. 4. Lattice parameters *a*, *c* for Ga(III) and *a* for Ga(II) crystalline structures determined by EDXD patterns at room temperature and compared with previous results (Ref. 7).

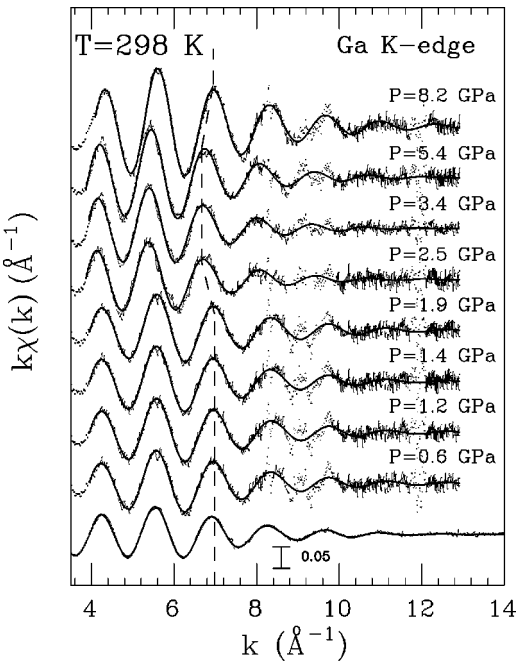

FIG. 5. Room temperature experimental XAS signals compared with best-fit calculated spectra for liquid and solid Ga at different pressures.

On increasing the temperature up to 378 K, large modifications in the XAS $\Delta\alpha$ difference signals have been found between 4.7 and 5.5 GPa (Fig. 2, central panel). These variations are due to the liquid-solid phase transition, in agreement with the phase diagram[4,5] as well as with present EDXD measurements showing the disappearance of the liquid $S(q)$ above 5 GPa. The phase transition *l*-Ga(III) is found at a pressure of about 5.4 GPa (at 378 K). Tiny changes appearing in the XAS spectra above this pressure suggest that no further solid-solid transitions take place in 5.5–11.8 GPa pressure range. The EDXD patterns collected in the solid region (5.5–14 GPa pressure range) show Bragg peaks assigned to the Ga(III) (101) and (110) interplanar distances only above 11 GPa. Numerical values for the lattice parameters are reported in Table I.

Finally, at 498 K (Fig. 2, right panel) we have found an appreciable difference between the absorption coefficients at 9 and 11 GPa certainly related to the liquid-solid transition. This transition is confirmed by EDXD data which shows the disappearance of the liquid $S(q)$ at 10.2 GPa but no evidence for Bragg peaks. We were not able to reconstruct the crystalline structure which is likely to be again Ga(III) as found at lower temperatures.[4,5]

Changes in the shape of experimental XAS data related to structural variations are better visualized looking at the $k\chi(k)$ XAS structural signals (where k is the wave vector of the photoelectron). Experimental XAS $k\chi(k)$ structural signals of solid and liquid Ga at room temperature are presented in the whole pressure range in Fig. 5. The lower most signal was collected at $T\sim 310$ K and $P\sim 0$ GPa using a conventional step-to-step XAS spectrometer.

The dashed line around $k\sim 7$ Å^{-1} is only a guide to the eye and allows us to highlight the clear changes of the oscillation frequency, related to modifications of the first-

TABLE I. Lattice parameters determined by EDXD patterns for solid gallium as a function of pressure.

T (K)	P (GPa)	Phase	$a_{(\mathrm{GaII})}$ (Å)	$a_{(\mathrm{GaIII})}$ (Å)	$c_{(\mathrm{GaIII})}$ (Å)
298(5)	5.7(1)	Ga(II)	5.745±0.008		
	8.6(1)	Ga(II)	5.695±0.008		
	10.7(1)	Ga(II)	5.648±0.008		
	14.0(1)	Ga(II)+Ga(III)	5.588±0.008		4.303±0.006
	17.0(1)	Ga(II)+Ga(III)	5.542±0.008	2.685±0.009	4.302±0.006
	19.0(1)	Ga(III)		2.681±0.009	4.172±0.005
	20.7(1)	Ga(III)		2.697±0.009	4.162±0.005
	23.3(1)	Ga(III)		2.667±0.009	4.120±0.005
	25.5(1)	Ga(III)		2.659±0.009	4.096±0.005
	29.8(1)	Ga(III)		2.636±0.009	4.029±0.005
378(5)	12.0(1)	Ga(III)		2.754±0.009	4.297±0.006
	14.0(1)	Ga(III)		2.733±0.009	4.284±0.006

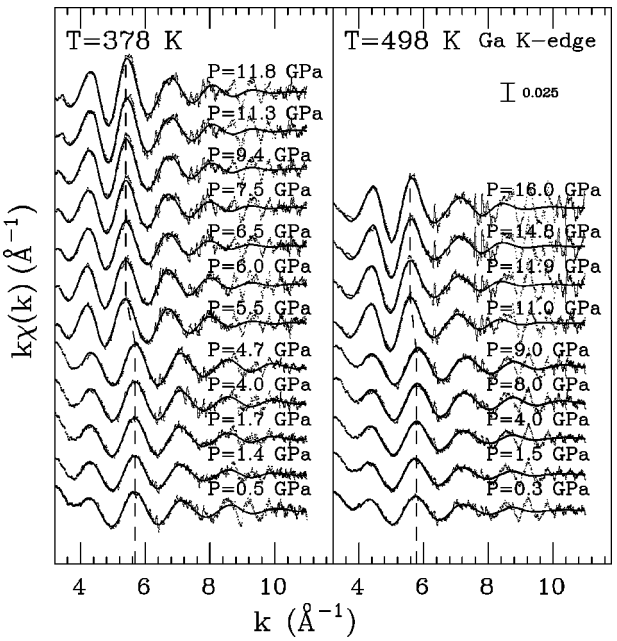

FIG. 6. Experimental XAS signals compared with best-fit calculated spectra for liquid and solid Ga as function of pressure at 378 (left panel) and 498 K (right panel).

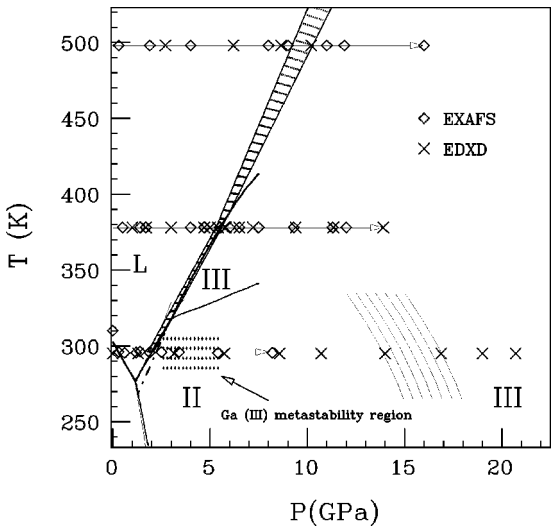

FIG. 7. Extension of Ga phase diagrams reported in Refs. 1,4 taking in account our new EDXD and XAS dispersive measurements. The dashed region at high temperature indicates the uncertainty in the liquid-Ga(III) coexistence line.

neighbor distances, obtained above $P=1.9$ and 5.4 GPa. The first sudden variation is obviously related to the liquid-solid phase transition occurring at about 2.0 GPa ($T\sim 298$ K). The liquid-solid transition is revealed both by the enhancement of the amplitude and by the change of frequency of the XAS spectra. A further frequency shift of the XAS signal of the solid phase as a function of pressure above 5.4 GPa has been discovered. This second change obtained is not expected because Ga(II) is supposed to be a stable phase up to about 15 GPa at room temperature.

Experimental XAS $k\chi(k)$ structural signals of solid and liquid Ga at 378 and 498 K are shown in Fig. 6 as a function of pressure. The structural transitions corresponding to an evident change of frequency of the XAS spectra occur above 4.7 and 9.0 GPa at $T\sim 378$ and 498 K, respectively. The vertical lines drawn in Fig. 6 are a guide to the eye which helps to better visualize the frequency shift.

In Fig. 7, the whole set of new measurements presented in this paper is reported and the limits of the diagram shown in Fig. 1 have been extended to include present limiting pressures and temperatures. The dotted region depicted in Fig. 7 in the 2.5–5.4 GPa pressure range at room temperature indicates a metastability region where gallium has been found to crystallize in different solid phases,[1] including the Ga(III) one, depending on the thermal and pressure history. In the present experiment we have not been able to detect any diffraction peak in that pressure range, however XAS data are compatible with the local environment typical of the Ga(III) phase (see next section).

In the high-temperature part of the phase diagram, the liquid-solid Ga (III) phase transition is placed in the 5.4(1)–5.5(1) GPa and 9.0(1)–10.2(1) GPa pressure ranges at 378 and 498 K, respectively. The dashed oblique lines indicate the uncertainty in the liquid-solid coexistence curve.

Finally, the high-pressure side of the phase diagram substantially confirms the previous results obtained in Ref. 7. Curves in the 14–17 GPa pressure range include a region where both Ga(II) and Ga(III) typical Bragg peaks have been found. In this work we provide an estimate of the lattice parameters of both phases in the coexistence region (see Fig. 4 and Table I).

IV. AVERAGE LOCAL STRUCTURE IN HIGH-PRESSURE PHASES

A. XAS data analysis of solid gallium

Data analysis has been carried out using the GNXAS package.[26] Phase shifts for photoabsorber and backscatterer atoms have been calculated for crystalline gallium structures using tangent muffin-tin spheres. The relevant $\gamma^{(2)}$ (two-body) and $\gamma^{(3)}$ (three-body) multiple scattering signals have been calculated.[26] Fitting was performed directly on the absorption data without any noise filtering or preliminary background subtraction. The dominant contribution is always the first-neighbor two-atom $\gamma^{(2)}$ signal even at high pressure, due to the relatively large structural disorder. Double-electron KM-type contributions were found in Ga (Ref. 27) and have been properly considered in the present data analysis. The importance of accounting for double-electron excitations has been widely emphasized elsewhere.[32–34] If not properly considered, these additional structures determine evident distortions of the $\chi(k)$ signal, which generate very short-distance Fourier transform (FT) peaks without structural meaning.

Data analysis of solid Ga at high pressure was performed using different models for the local structure: Ga III, Ga II and a simple twelve neighbors shell model (asymmetric Γ-like distribution, see Refs. 35–37, and references therein).

The latter model is defined by the expression

$$n(r)=\frac{2N}{\sigma|\beta|\Gamma(4/\beta^2)}\left(\frac{4}{\beta^2}+\frac{2(r-R)}{\sigma\beta}\right)^{4/\beta^2-1}\times\exp\left[-\left(\frac{4}{\beta^2}+\frac{2(r-R)}{\sigma\beta}\right)\right], \quad (1)$$

where the radial distribution $n(r)$ depends upon three structural quantities:[35] the average bond length R, the bond variance σ^2, and the skewness β [$N=\int n(r)dr=12$].

Detailed analysis of the XAS results, reported in Ref. 38, shows that the local structure of solid Ga up to 5.4 GPa is not compatible with Ga II (eight first neighbors at ~2.78 Å and four at about 3.33 Å, $P=2.6$ GPa, 313 K) while it is in substantial agreement with that of Ga III (four first-neighbor atoms around 2.81 Å and eight around 2.98 Å, 2.8 GPa, 298 K). This result is in accord with previous observations by Bosio[1] where gallium was found to crystallize in different solid phases in the Ga II stability domain (see Fig. 7, dotted region). At higher pressures ($P>5.4$ GPa) we have found that the local structure is compatible with the Ga II model. This is in agreement with the observation of the Ga II Bragg peaks identified in the EDXD patterns above 5.7 GPa (see previous section), as well as with the observed change in the XAS spectra between 5.4 and 8.2 GPa.

We have verified that the Γ-like asymmetric model is able to reproduce the XAS experimental data at high pressure and temperature within the noise. The short-range radial distribution function defined by Eq. (1) has been found to reproduce that of the known crystalline phases using always the same parametrization in the various thermodynamic P, T conditions presented in this work. The best-fit calculated XAS signals using the Γ-like asymmetric model (thick lines) are compared with experimental data (thin lines) at room and higher temperatures in Figs. 5 and 6, respectively. Experimental points shown as small dots in Fig. 5 (see region around 9 $Å^{-1}$) contain spurious structures related to weak Bragg peaks coming from the diamonds of the cell and have not been considered in the refinement process. The good agreement between theoretical and experimental signals is evident in the whole pressure and temperature ranges.

XAS data analysis allowed us to obtain the best-fit values of the structural parameters R, σ^2, and β defining the Γ-like distribution. The results of the fitting procedure are reported in Table II. At a given temperature, the average bondlength R decreases by increasing the pressure following the natural contraction of the unit cell. Conversely, at a given pressure the average first-neighbor distance slightly increases with temperature (thermal expansion). The bond length variance σ^2, associated to thermal and static configurational disorder, shows a dramatic temperature dependence. In the present pressure range, the decrease of the variance upon application of pressure is slightly less important. The skewness β, associated with an asymmetry of the radial distribution (i.e., anharmonic terms), increases with temperature and decreases with pressure. The increase of β is particularly evident at $T=498$ K. The effect on the XAS data is a decrease of the leading frequency on increasing the temperature that, as it has been shown in several recent publications (see, for example, Refs. 36–39) is related to the asymmetry of the first-neighbor distribution and not to an anomalous decrease of the average distance.

TABLE II. First-shell parameters determined by XAS data analysis using the Γ-like asymmetric model for solid gallium at room temperature, $T\sim398$ and 498 K as a function of pressure.

T (K)	P (GPa)	R (Å)	σ^2 ($Å^2$)	β
298(5)	2.5(1)	2.893(5)	0.035(2)	0.40(5)
	3.4(1)	2.891(5)	0.033(2)	0.39(5)
	5.4(1)	2.863(5)	0.030(2)	0.32(5)
	8.2(1)	2.822(5)	0.029(2)	0.59(5)
398(5)	5.5(1)	2.925(5)	0.044(2)	0.49(5)
	6.0(1)	2.914(5)	0.042(2)	0.46(5)
	6.5(1)	2.887(5)	0.040(2)	0.30(5)
	7.5(1)	2.877(5)	0.038(2)	0.25(5)
	9.4(1)	2.852(5)	0.035(2)	0.16(5)
	11.3(1)	2.840(5)	0.034(2)	0.15(5)
	11.8(1)	2.835(5)	0.033(2)	0.14(5)
498(5)	11.0(1)	2.849(5)	0.048(2)	0.56(5)
	11.9(1)	2.843(5)	0.048(2)	0.54(5)
	14.8(1)	2.810(5)	0.044(2)	0.41(5)
	16.0(1)	2.792(5)	0.041(2)	0.35(5)

Present XAS structural data on solid gallium can be better rationalized by reconstructing the corresponding radial distribution $n(r)$ functions. Even in presence of mixture of phases the short-range $n(r)$ presented in Fig. 8 have the precise physical meaning of measuring the average local structure of solid Ga in that range of pressure. The $n(r)$ reconstruction is very accurate in the short-range side of the peak but the uncertainty increases at longer distances.

In Fig. 8 we present the complete set of $n(r)$ functions for solid Ga as a function of pressures and temperatures, derived using the asymmetric Γ-like twelve-neighbors distribution. The position of the maximum is shortened from 2.84 to about 2.75 Å on increasing the pressure from 2.5 to 8.2 GPa. The peak height increases from about 25.9 to 29 in the same pressure range. While the amplitude increase is roughly proportional to the pressure change, the shape of the distribution drastically changes above 5.4 GPa. As discussed above, the XAS spectra in an intermediate pressure range 2.5–5.4 GPa are compatible with a Ga III structure while at 8.2 GPa the average local structure is compatible with that of Ga II, observed by EDXD (see Sec. III). For the high-temperature data, we present the $n(r)$ functions calculated in the 5.5(1)–11.8(1) GPa (Fig. 8, middle panel) and 11.0(1)–16.0(1) GPa (Fig. 8, right panel) pressure ranges at 378 and 498 K, respectively. On increasing the pressure the height of the first $n(r)$ peak increases while the mean value of the distance decreases (see symbols in Fig. 8). At the same time, the foot and the most probable value of the distribution functions shift toward shorter distances on increasing the temperature. A longer tail indicating a larger asymmetry is also easily observed increasing the temperature.

B. XAS data analysis of liquid gallium

The most important contribution to the XAS structural signal is associated with the first-neighbor peak and therefore

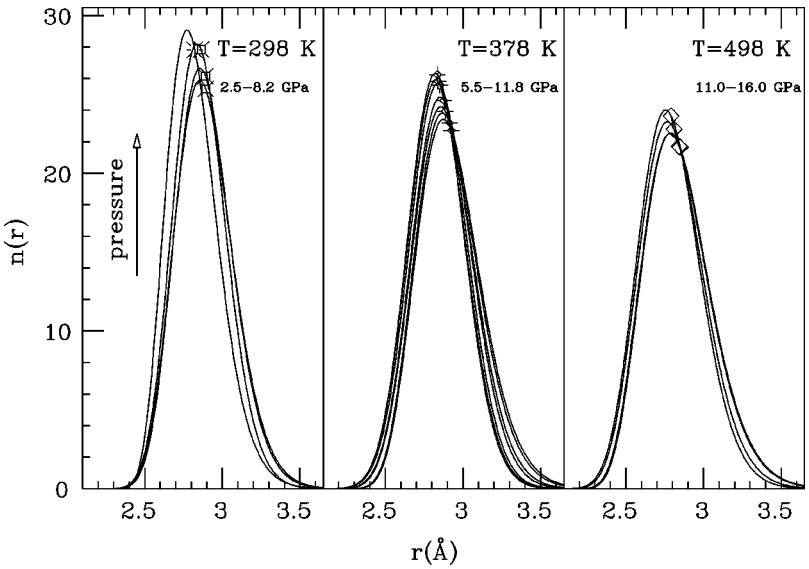

FIG. 8. Reconstruction of $n(r)$ radial distribution functions by XAS data analysis for solid gallium at high temperature. Left panel: $n(r)$ functions determined at room temperature in the 2.5–8.2 GPa pressure range ($P=2.5$, 3.4, 5.4, and 8.2 GPa). Middle panel: $n(r)$ functions calculated in the 5.5–11.8 GPa at 378 K ($P=5.5$, 6.0, 6.5, 7.5, 9.4, 11.3, and 11.8 GPa). Right panel: $n(r)$ functions calculated in the 11.0–16.0 GPa pressure range at 498 K ($P=11$, 11.9, 14.8, and 16 GPa). Average values of first-shell interatomic distances are indicated by the symbols.

the $k\chi(k)$ is extremely sensitive to its shape. Several recent papers (see, for example, Refs. 29,35,36,39,40) have shown that it is convenient to decompose the $g(r)$ into a short-range peak and a long-range tail.[28] In this way the $g(r)$ long-range asymptotic behavior, obtained by $S(q)$ diffraction data or by computer simulations, is retained while the short-range part can be refined. Data analysis of XAS spectra of liquid gallium has been performed considering the constraints imposed by the long-range behavior of the $g(r)$ functions obtained from neutron and x-ray diffraction experiments.[9,10] A suitable decomposition of the $g(r)$ curve into a short-range peak and a long-range tail has been made. The first-neighbor peak of the $g(r)$ obtained by neutron diffraction has been modeled as a sum of two Γ-like[35] functions (see Fig. 9), due to its largely asymmetric shape. The decomposition of the first $g(r)$ peak into two components has been found to be necessary in *l*-Ga for achieving both an accurate reproduction of the original $g(r)$ and an optimal best fit of the XAS structural signal.

In Fig. 10 (left panel) the $k\gamma^{(2)}$ signals related to the Γ-like functions ($k\gamma_{\rm I}^{(2)}$ and $k\gamma_{\rm II}^{(2)}$), and the tail $k\gamma_T^{(2)}$ are shown for the spectrum at 1.9 GPa and room temperature. The total structural signal obtained by summing the three $k\gamma^{(2)}$ terms is compared with the experimental $k\chi(k)$ of *l*-Ga at various pressures. The amplitude and phase of the signal is almost exactly reproduced but, looking at the residual curve, a refinement is still necessary. The short-range refinement of *l*-Ga has been performed floating the parameters of the Γ-like distributions and considering the tail (Fig. 10, right panel). As shown in Ref. 28, a correct reconstruction of the short-range $g(r)$ can be performed only taking into account for the compressibility sum rule and asymptotic behavior at long distances. For the particular case of two Γ functions reproducing the first $g(r)$ peak the introduction of two constraints in the refinement process is required. The first one is the coordination number constraint $\Delta(N_1+N_2)=0$, and the second one is the constraint on the second moment of the distribution which corresponds to the equation $\Delta[N_1(R_1^2+\sigma_1^2)+N_2(R_2^2+\sigma_2^2)]=0$, where N_1, R_1, σ_1^2 and N_2, R_2, σ_2^2 are the parameters of two peaks, respectively.[28] By using these constraints, the shapes of the first and second peaks are not independent. XAS data analysis at room temperature has been performed using those constraints in the 0.6–1.9 GPa pressure range and the resulting best-fit calculated signals are in excellent agreement with the corresponding experimental signals as already shown in Fig. 5.

Structural data-analysis of *l*-Ga at high temperature has been performed using the same procedure used for the room-temperature data. In this case the decomposition of the $g(r)$ obtained from neutron diffraction experiments into a short-range part and a long-range tail has been made taking account of different macroscopic densities for each temperature in order to define the proper constraints for the coordination

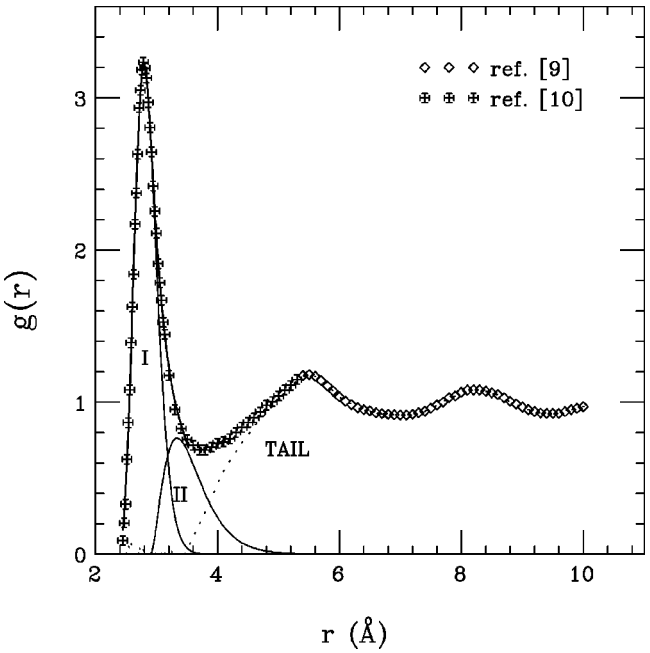

FIG. 9. Pair distribution function $g(r)$ as reported in Refs. 9,10. The decomposition of the first-neighbor peak into two Γ functions is shown (solid lines). The residual (tail) curve accounting for the medium and long-range correlations is also shown.

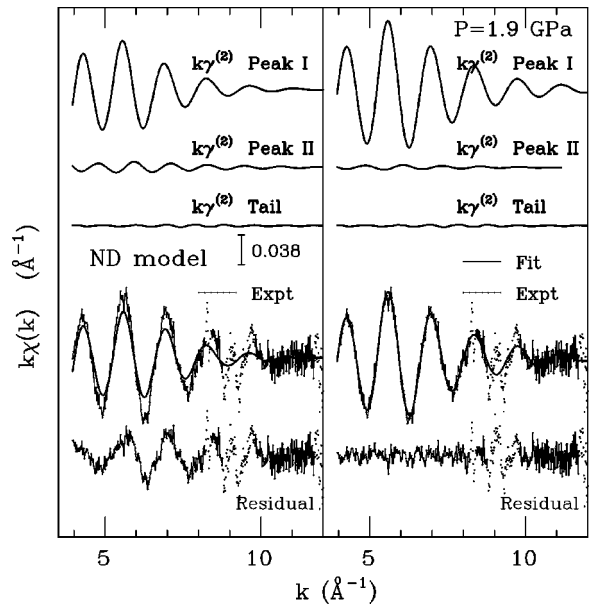

FIG. 10. Left panel: pair contributions $k\gamma^{(2)}$ associated with the two first-neighbors shells describing the first $g(r)$ peak and the long-range tail. The total $k\gamma^{(2)}$ signal is compared with the $k\chi(k)$ experimental spectrum of liquid Ga at 1.9 GPa. The residual curve indicates that a structural refinement is necessary. Right panel: Best-fit $k\gamma^{(2)}$ signals for the *l*-Ga $k\chi(k)$ spectrum at 1.9 GPa. The agreement with experimental data is excellent.

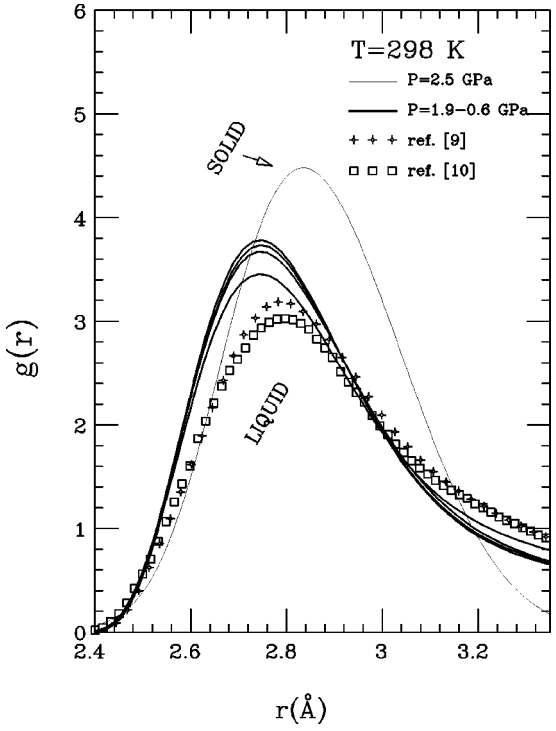

FIG. 11. Pair distribution functions $g(r)$ of *l*-Ga at $P=0.6$, 1.2, 1.4, and 1.9 GPa compared with data of Refs. 9,10 and a typical solid Ga first-shell peak reconstructed by XAS data analysis at room temperature and 2.5 GPa.

numbers. Realistic densities of *l*-Ga have been evaluated starting from the usual linear approximation for liquid metals: $\rho=\rho_m+\Lambda(T-T_m)$, where $\rho_m=6.103$ (10^3 Kg m^{-3}), $\Lambda=(\partial\rho/\partial T)_p=-6.2$ (10^{-1} Kg m^{-3}K^{-1}) (Ref. 41) and $T_m=302.9$ K. We did not consider variations of Λ as a function of temperature (and pressure) that we expect to be negligible in the present ranges. In Fig. 6 best-fit calculations (thick lines) are compared with the experimental spectra (thin lines) in the 0.5–4.7 GPa ($T=378$ K) and in 0.3–9.0 GPa pressure ranges ($T=498$ K). The good agreement between theoretical and experimental signals is evident.

C. XAS $g(r)$ reconstruction in liquid gallium

The pair distribution $g(r)$ functions have been reconstructed for liquid gallium starting from the structural parameters determined by means of XAS data analysis.[28,40,42] In Fig. 11 the pair distribution $g(r)$ functions calculated by XAS are shown for liquid Ga at room temperature. In the same figure, we also show the $g(r)$ functions at ambient pressure reported in Refs. 9,10 and a typical solid Ga first-shell peak (see Sec. IV A) for comparison. The typical error bar on the reconstructed $g(r)$ functions is of about 0.1 on the first-peak rise and increases for longer distances (see Refs. 29,39, and references therein). The height of the first-neighbor peak in liquid Ga increases slightly with pressure while no detectable distance changes are found. The $g(r)$ peak height increases from about 3.5 (0.6 GPa) to 3.8 (1.9 GPa) at 298 K. The position of the maximum is at about 2.76 Å. In solid Ga at moderate pressure (2.5 GPa), shown for comparison in Fig. 11, the peak is shifted to longer distances. The slight pressure dependence of the first-neighbor peak in liquid Ga corresponds to amplitude variations in the original XAS signals (see also Refs. 43,44).

The height of the first-neighbor peak is affected both by temperature and pressure parameters. In Fig. 12 we report the short-range $g(r)$ functions for *l*-Ga as a function of temperature at given pressures. The peak height decreases from about 3.8 to 3.0 temperature from 298 to 498 K at about 1.5 GPa (right panel). At lower pressures (around 0.5 GPa) the same trend is observed (decrease from 3.5 to 2.9 increasing the temperature, see left panel). Looking at Fig. 12 we observe that the shape of the pair distribution function is strongly affected by varying the temperature. The strong dependence on the temperature was previously observed by neutron diffraction measurements at ambient pressure. In fact, comparing the $g(r)$ at room temperature and at about 959 K at ambient pressure (see Fig. 12),[10] one can see that the first rise of the $g(r)$ moves toward shorter distances, the height decreases dramatically, and an increased asymmetry of the distribution is obtained. We observe a similar behavior on our $g(r)$ distributions at higher pressure. The position of the peak maximum does not move appreciably as a function of temperature in agreement with previous findings.[21]

In Fig. 13 we present our reconstructed short-range $g(r)$ functions for *l*-Ga as a function of pressure at given temperatures. A slight enhancement of the peak is obtained increasing the pressure. The $g(r)$ peak intensity increases from about 3.1 (0.5 GPa) to 3.3 (4.7 GPa) at 378 K (left panel) and from about 2.8 (0.3 GPa) to 3.0 (9.0 GPa) at 498 K (right panel). Moreover, the position of the maximum of the distri-

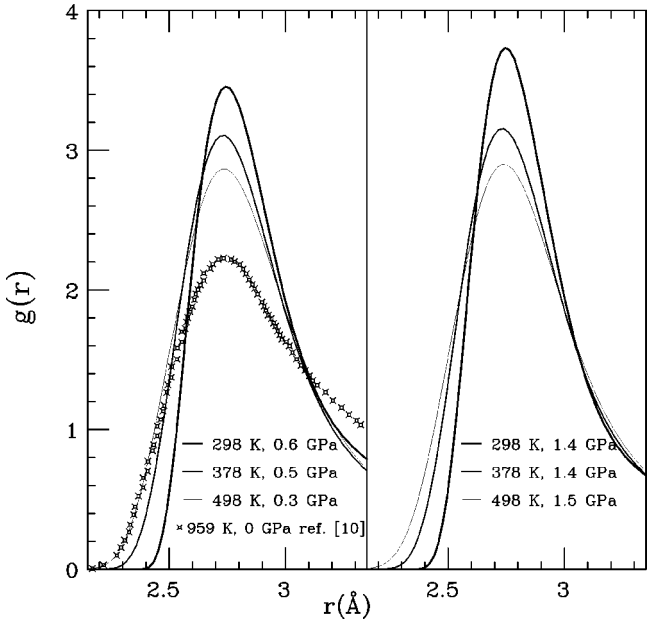

FIG. 12. Left panel: Pair distribution functions $g(r)$ reconstructed by XAS data analysis for *l*-Ga at 298 K and 0.6 GPa, 378 K and 0.5 GPa, 498 K and 0.3 GPa. The $g(r)$ function at ambient pressure and $T=959$ K reported in Ref. 10 is also shown for comparison. Right panel: Pair distribution functions of *l*-Ga at 298 K and 1.4 GPa, 378 K and 1.4 GPa, 498 K and 1.5 GPa.

bution moves toward shorter distances from about 2.72 (0.5 GPa) to 2.70 (4.7 GPa) (see left panel in Fig. 13) at 378 K and from about 2.72 (0.3 GPa) to 2.68 (9 GPa) (see right panel in the same figure) at 498 K. The slight decrease of the distance on increasing the pressure is in qualitative agreement with previous results obtained using x-ray diffraction.[22]

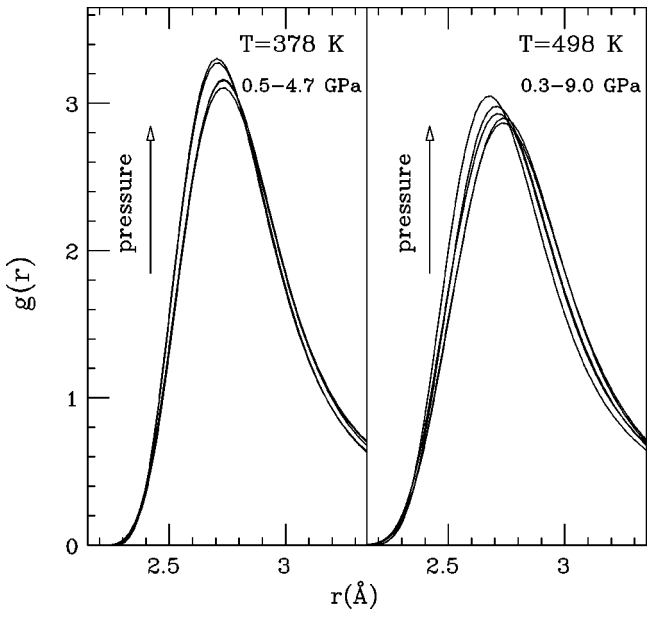

FIG. 13. Pair distribution functions $g(r)$ calculated by XAS data analysis for *l*-Ga shown as a function of pressure at $T=378$ K (left panel) and 498 K (right panel).

V. CONCLUSIONS

A detailed investigation of the high-pressure and high-temperature *K*-edge x-ray absorption spectra of solid and liquid gallium has been carried out. Phase transitions occurring in the 0-16 GPa range of pressures under investigation are detected at three different temperatures. The Ga phase diagram has been extended at high temperature showing the liquid to solid phase transition at about 500 K occurring in the 9–10.2 GPa pressure range.

EDXD patterns have been also collected confirming the occurrence of phase transitions at the same pressures found using the XAS technique. Ga(II) and Ga(III) cell parameters, identified taking into account previously published diffraction data, have been measured up to about 30 GPa. By combining XAS and EDXD data we have shown that at room temperature liquid Ga does not nucleate into the accepted stable phase Ga(II) by increasing the pressure. This phase is observed at higher pressures ($P\sim5.7$ GPa) and a second transition from Ga(II) to Ga(III) is obtained above 10.7 GPa in a range of about 4 GPa.

XAS data analysis has been performed using the advanced GNXAS multiple-scattering method. XAS data of solid Ga have been found to be particularly sensitive to the short-range side of the first-neighbor distribution. A Γ-like asymmetric model depending on the average first-neighbor bond length R, bond distance variance σ^2 and skewness β has been found to describe accurately the first-neighbor distribution. The trend of the R, σ^2, β structural parameters are presented in wide pressures and temperatures ranges. Reconstructed radial distribution functions $n(r)$ have been found to be largely asymmetric especially near the melting curves. The increased asymmetry of the distribution, associated with the increase of vibrational amplitudes and anharmonic contributions, has been shown to explain the lowering of the leading XAS oscillation in presence of the thermal expansion at a given pressure.

XAS data analysis of liquid Ga has been performed using constraints provided by neutron, x-ray diffraction, and density data. The short-range pair distribution function $g(r)$ for *l*-Ga has been reconstructed for the first time in a wide range of pressures and temperatures. The local average structure of *l*-Ga under pressure (up to 1.9 GPa) at room temperature is found to be compatible with that of *l*-Ga at ordinary pressure measured by neutron diffraction. The maximum of the first-neighbor distribution is slightly shifted toward short distances and its height increases with the pressure. At higher temperatures, *l*-Ga has been measured up to 9 GPa and both a slight contraction of distances and enhancement of the first-neighbor peak have been observed. By increasing the temperature the height of the first-neighbor peak decreases while the first rise in the $g(r)$ functions moves to shorter distances showing a modification in the average local structure for the liquid phase as function of temperature, in agreement with previous results obtained at ambient pressure.

The accurate determination of short-range pair distribution functions presented in this work can stimulate new theoretical and computational studies of short-range potentials

and electronic properties for gallium under extreme conditions. Present results show also the potentialities of the x-ray absorption spectroscopy in the study of polymorphic metals in high-pressure and/or high-temperature conditions. XAS results are found to be fully compatible with x-ray diffraction data and therefore the technique is shown to provide useful complementary information about the average structure in ordered and disordered phases.

[1] L. Bosio, J. Chem. Phys. **68**, 1221 (1978).
[2] L. Bosio, R. Cortes, A. Defrain, and G. Folcher, J. Chim. Phys. Phys.-Chim. Biol. **70**, 357 (1973).
[3] A. Di Cicco, Phys. Rev. Lett. **81**, 2942 (1998).
[4] A. Jayaraman, W. Klement, R.C. Newton, and G.C. Kennedy, J. Phys. Chem. Solids **24**, 7 (1963).
[5] E. Yu Tonkov, *High Pressure Phase Transformations. A Handbook* (Gordon and Breach, London, 1992).
[6] C.E. Weir, G.J. Piermarini, and S. Block, J. Chem. Phys. **54**, 2768 (1964).
[7] O. Schulte and W.B. Holzapfel, Phys. Rev. B **55**, 8122 (1997).
[8] T. Kenichi, K. Kazuaki, and A. Masao, Phys. Rev. B **58**, 2482 (1998).
[9] A.H. Narten, J. Chem. Phys. **56**, 1185 (1972).
[10] M.C. Bellissent-Funel, P. Chieux, D. Levesque, and J.J. Weis, Phys. Rev. A **39**, 6310 (1989).
[11] A. Bererhi, L. Bosio, and R. Cortes, J. Non-Cryst. Solids **30**, 273 (1979).
[12] A. Bererhi, A. Bizid, L. Bosio, R. Cortes, A. Defrain, and C. Segaud, J. Phys. Colloq. **41**, 218 (1980).
[13] G. Gong, G.L. Chiarotti, M. Parrinello, and E. Tosatti, Europhys. Lett. **21**, 469 (1993).
[14] J.M. Holender, M.J. Gillan, M.C. Payne, and A.D. Simpson, Phys. Rev. B **52**, 967 (1995).
[15] C. Regnaut, J.P. Badiali, and M. Dupont, Phys. Lett. **79A**, 245 (1979); **75A**, 516(E) (1979).
[16] S.K. Lai, W. Li, and M.P. Tosi, Phys. Rev. A **42**, 7289 (1990).
[17] J. Hafner and W. Jank, Phys. Rev. B **42**, 11 530 (1990).
[18] S. Tsay, Phys. Rev. B **48**, 5945 (1993).
[19] S. Tsay, Phys. Rev. B **50**, 103 (1994).
[20] S. Tsay and S. Wang, Phys. Rev. B **50**, 108 (1994).
[21] K. Tamura and S. Hosokawa, J. Non-Cryst. Solids **156-158**, 650 (1993).
[22] K. Tsuji, J. Non-Cryst. Solids **117-118**, 27 (1990).
[23] A. Di Cicco, A. Filipponi, J.P. Itié, and A. Polian, Phys. Rev. B **54**, 9086 (1996).
[24] J.P. Itié, A. Polian, D. Martinez, V. Briois, A. Di Cicco, A. Filipponi, and A. San-Miguel, J. Phys. IV **C2**, 31 (1997).
[25] U. Buontempo, A. Filipponi, D. Martínez-García, P. Postorino, M. Mezouar, and J.P. Itié, Phys. Rev. Lett. **80**, 1912 (1998).
[26] A. Filipponi, A. Di Cicco, and C.R. Natoli, Phys. Rev. B **52**, 15 122 (1995); **52**, 15 135 (1995).
[27] A. Di Cicco and A. Filipponi, J. Non-Cryst. Solids **156-158**, 102 (1993).
[28] A. Filipponi, J. Phys.: Condens. Matter **6**, 8415 (1994).
[29] A. Di Cicco, M. Minicucci, and A. Filipponi, Phys. Rev. Lett. **78**, 460 (1997).
[30] E. Dartyge, C. Depautex, J.M. Dubuisson, A. Fontaine, A. Jucha, and G. Tourillon, Nucl. Instrum. Methods Phys. Res. A **246**, 452 (1986).
[31] H. Tolentino, E. Dartyge, A. Fontaine, and G. Tourillon, J. Am. Ceram. Soc. **21**, 15 (1988).
[32] P. D'Angelo, A. Di Cicco, A. Filipponi, and N.V. Pavel, Phys. Rev. A **47**, 2055 (1993).
[33] A. Filipponi and A. Di Cicco, Phys. Rev. B **49**, 12 564 (1994).
[34] A. Filipponi and A. Di Cicco, Phys. Rev. A **52**, 1072 (1995).
[35] A. Filipponi and A. Di Cicco, Phys. Rev. B **51**, 12 322 (1995).
[36] A. Di Cicco, M.J. Rosolen, R. Marassi, R. Tossici, A. Filipponi, and J. Rybicki, J. Phys.: Condens. Matter **8**, 10 779 (1996).
[37] M. Minicucci and A. Di Cicco, Phys. Rev. B **56**, 11 456 (1997).
[38] L. Comez, Ph.D. thesis, Dottorato di Ricerca, Università di Camerino, Italy, 2001.
[39] A. Di Cicco, M. Taglienti, M. Minicucci, and A. Filipponi, Phys. Rev. B **62**, 12 001 (2000).
[40] A. Di Cicco, G. Aquilanti, M. Minicucci, A. Filipponi, and J. Rybicki, J. Phys.: Condens. Matter **11**, L43 (1999).
[41] T. Iida and R. I. L. Guthrie, *The Physical Properties of Liquid Metals* (Clarendon Press, Oxford, 1993).
[42] A. Di Cicco and A. Filipponi, J. Non-Cryst. Solids **205-207**, 304 (1996).
[43] A. Di Cicco, L. Comez, J. P. Itié, and A. Polian, in *Science and Technology of High Pressure*, Proceedings of the AIRAPT-17 International Conference, 1999, edited by M. H. Manghnani, W. J. Nellis, and M. F. Nicol (Universities Press, Hyderabad, India, 2000), Vol. 1, p. 452.
[44] L. Comez, A. Di Cicco, M. Minicucci, R. Tossici, J. P. Itié, and A. Polian, J. Synchrotron Radiat. **8**, 776 (2001).